Differential flatness-based robust control of mobile robots in the presence of slip

Article *in* The International Journal of Robotics Research · April 2011

DOI: 10.1177/0278364910385586 · Source: DBLP

2 authors:

Ji-Chul Ryu
Northern Illinois University
31 PUBLICATIONS **410** CITATIONS

SEE PROFILE

Sunil K. Agrawal
Columbia University
466 PUBLICATIONS **9,512** CITATIONS

SEE PROFILE

Preprint. Published in *The International Journal of Robotics Research*, Vol. 30. No. 4, pp. 463-475, 2011

Differential Flatness-based Robust Control of Mobile Robots in the Presence of Slip

Ji-Chul Ryu, Ph.D.
Mechanical Systems Laboratory
University of Delaware
Newark, DE 19716
Email: jcryu@udel.edu

Sunil K. Agrawal, Ph.D., Professor
Mechanical Systems Laboratory
University of Delaware
Newark, DE 19716
Email: agrawal@udel.edu

***Abstract*—Slip between the ground and wheel often cannot be avoided in most applications of mobile robots. However, a majority of controllers developed so far make no-slip assumption with nonholonomic constraints. To achieve desired performance in the presence of slip, controllers that are robust to slip are required.**

In this paper, we discuss robust trajectory-tracking control for a differentially driven two-wheeled mobile robot. The structure of a differential flatness controller, which has shown distinctive advantages providing an integrated framework for planning and control, is extended to account for slip disturbances. It is shown that the differential flatness framework can be extended to develop a robust controller based on dynamic as well as kinematic model with slip.

Simulation results for both kinematic and dynamic controllers are presented to demonstrate the effectiveness of the robust controllers. Experiments with the kinematic controller which is suited to typical laboratory and field mobile robots were conducted to validate the proposed robust controller. The simulation and experimental results show that the proposed robust controllers are effective in the presence of slip.

I. Introduction

Wheeled mobile robot is an active area of robotics research due to the practical importance of its applications. Control algorithms for various mobile robots such as differentially driven two-wheeled (Samson and Ait-Abderrahim 1991; Fierro and Lewis 1997; Pathak and Agrawal 2005), car-like (Murray and Sastry 1991; Laumond 1998), tractor-trailer systems (De-Santis 1994; Rouchon et al. 1993; Ryu and Agrawal 2008) and others have been extensively studied in the literature. Among these control algorithms, it has been shown that the differential flatness theory (Fliess et al. 1995) can remarkably simplify trajectory planning and controller design of such robotic systems if the system has the flatness property (Sira-Ramirez and Agrawal 2004; D'Andrea-Novel et al. 1995).

With the flatness property, states and inputs can be parameterized by a finite set of differentially independent variables, called flat outputs, and their finite number of derivatives. The number of flat outputs equals to the number of control inputs. From a planning point of view, the most important aspect of the differential flatness is that desired trajectories can be planned easily in the flat output space. The trajectories planned in the flat output space are automatically consistent with the system's dynamic equations. The flat output trajectories can then be mapped onto the original states and inputs. In addition, exponentially stabilizing controllers can be easily developed for the system since the system is represented by a linear chain of integrators in the flat output space.

In a majority of the research on control of wheeled mobile robots including the references cited above, nonholonomic constraints have been used, which result from assuming no-slip between the ground and the wheels. However, in most real applications, slip exists due to various reasons such as uneven terrain, high speed, or slippery ground condition. As a result, the controllers that are based on no-slip model, even if they are feedback controllers, may not work properly. To cope with this problem, robust controllers have been developed. For two-wheeled mobile robots, robust controllers that can cope with slip were proposed in Dixon et al. (2000b) and Zhu et al. (2006) using dynamic oscillators and transverse functions, respectively. For car-like mobile robots, a linearized kinematic model-based robust controller was presented in Fang et al. (2006). Whereas these controllers consider only the kinematic model, robust controllers based on dynamic model are preferable in order to deal with dynamic effects. The robust controller in Leroquais and D'Andrea-Novel (1996) was developed based on the singular perturbation approach and another robust controller was designed at the dynamic level using backstepping method (Wang et al. 2004). In this reference, the controller assumes that the slip velocity exists only in the lateral direction. The backstepping approach was also used in the controllers presented in Dixon et al. (2000a) and Kim et al. (2003). Feedback linearization based robust control was used for a four-wheel driven mobile robot (Bendtsen et al. 2002). Sliding mode control is another popular method for developing controllers that are robust to model uncertainty and external disturbance (Yang and Kim 1999; Corradini and Orlando 2001). However, in these studies, the dynamic models explicitly assume that the nonholonomic constraints are always met. In Zhang et al. (2003), the authors adopted a tire friction model to derive a dynamic model and designed a robust controller for a two-wheeled mobile robot. Another approach to handle the slip relies on estimating the slip in real-time using gyros and accelerometers (Seyr and Jakubek 2006; Low and Wang 2007) to compensate for it.

While the application of differential flatness has been inves-

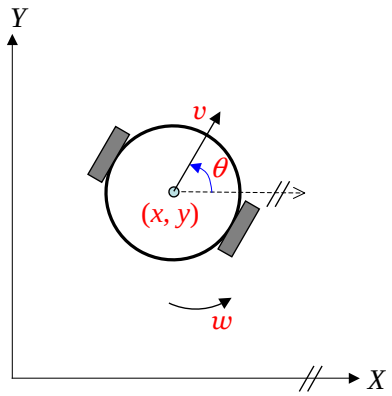

Fig. 1. A two-wheeled differentially driven mobile robot described by three configuration variables x, y, θ with no slip on the wheels.

tigated in the literature in the absence of slip of the wheels, the main contributions of this paper are: (i) it is shown that it is possible to extend the differential flatness structure to develop a robust controller based on the dynamic model as well as the kinematic model in the presence of slip; and (ii) experimental validation of the differential flatness based robust controller.

In this paper, we first present the kinematic model with all possible slips of the wheels. We then derive the dynamic model with the slip disturbances starting from the slip-kinematic model. We then present designs of robust controllers based on the slip-kinematic and slip-dynamic models using the framework of differential flatness. The kinematic controller is valuable since inputs to a kinematic model are the motor speeds, which are suited to typical laboratory and field mobile robots that only allow speed commands like iRobot's Magellan Pro used in this study. Also, to some extent, the kinematic model with the slip disturbances can account for external dynamic forces, unmodeled dynamics, and/or parametric uncertainty. For these reasons, we present the experimental results of the kinematic controller.

The rest of this paper is organized as follows: In Section II, differential flatness properties of the kinematic and dynamic models of the differentially driven two-wheeled robot with no slip are reviewed. In Section III, kinematic and dynamic models of the robot in the presence of slip are derived . Robust control design is addressed in Section IV. Simulation and experimental results are presented in Sections V and VI, respectively. Finally, concluding remarks are given at the end of the paper.

II. Review of No-slips Model and Differential Flatness

In this section, we review the no-slip models and their differential flatness. The steps outlined in this section in order to obtain the equivalent governing equations in the flat output space will also be used in the design of the robust controller. Desired trajectories for the mobile robot to track will also be planned based on these no-slip models.

A. Kinematic Model with No Slip

In this section, we derive the kinematic model of a differentially driven two-wheeled mobile robot shown in Fig. 1. In Cartesian coordinates, the system's configuration is given by

$$\mathbf{q} = [x, y, \theta]^T, \tag{1}$$

where (x, y) is the center position of the robot and θ is the orientation with respect to the X-axis.

From the assumption of no-slip condition on the wheels, the nonholonomic constraint is given by

$$\mathbf{C}(\mathbf{q})\dot{\mathbf{q}} = \mathbf{0}, \tag{2}$$

where

$$\mathbf{C}(\mathbf{q}) = [\sin\theta, -\cos\theta, 0]. \tag{3}$$

With a matrix $\mathbf{S}(\mathbf{q})$ that spans the null space of $\mathbf{C}(\mathbf{q})$, it is possible to represent the kinematic model of the mobile robot as

$$\dot{\mathbf{q}} = \mathbf{S}(\mathbf{q})\boldsymbol{\nu}, \tag{4}$$

where

$$\mathbf{S}(\mathbf{q}) = \begin{pmatrix} \cos\theta & 0 \\ \sin\theta & 0 \\ 0 & 1 \end{pmatrix}, \boldsymbol{\nu} = [v \;\; w]^T. \tag{5}$$

Here, v and w represent the forward and angular velocities of the mobile robot, respectively. Equation (4) can be rewritten as

$$\begin{aligned} \dot{x} &= v\cos\theta, \\ \dot{y} &= v\sin\theta, \\ \dot{\theta} &= w. \end{aligned} \tag{6}$$

To outline how the kinematic model of the two-wheeled mobile robot is differentially flat, we choose the flat outputs to be the Cartesian position of the center of the robot (x, y). Input prolongation is used to create a diffeomorphism between the original states and the flat outputs and their derivatives. This property is used in planning of desired trajectory and in design of control laws to track the trajectory.

On applying one prolongation of v, i.e., by considering v an additional state, the prolonged systems is given by

$$\begin{aligned} \dot{x} &= v\cos\theta, \\ \dot{y} &= v\sin\theta, \\ \dot{v} &= \bar{u}_1, \\ \dot{\theta} &= \bar{u}_2. \end{aligned} \tag{7}$$

Here, $\bar{u}_1$, $\bar{u}_2$ are the new inputs for the extended system consisting of four states and satisfy

$$\bar{u}_1 = \dot{v}, \;\; \bar{u}_2 = w. \tag{8}$$

By choosing the flat outputs $\mathbf{F} = [F_1, F_2]^T = [x, y]^T$, all state variables and inputs can be expressed in terms of the flat outputs and their derivatives. With $(x, y) = (F_1, F_2)$, their expressions are:

$$v = \sqrt{\dot{F}_1^2 + \dot{F}_2^2}, \;\; \theta = \tan^{-1}\left(\frac{\dot{F}_2}{\dot{F}_1}\right), \tag{9}$$

and the inputs $\bar{u}_1$, $\bar{u}_2$ can also be expressed as

$$\bar{u}_1 = \dot{v} = \frac{\dot{F}_1\ddot{F}_1 + \dot{F}_2\ddot{F}_2}{\sqrt{\dot{F}_1^2 + \dot{F}_2^2}}, \tag{10a}$$

$$\bar{u}_2 = \dot{\theta} = \frac{\dot{F}_1\ddot{F}_2 - \ddot{F}_1\dot{F}_2}{\dot{F}_1^2 + \dot{F}_2^2}. \tag{10b}$$

An invertible mapping between the inputs and higher derivatives of the flat outputs can be constructed by differentiating the flat outputs until an input appears, or it can also be equivalently constructed from Eq. (10). The mapping is given by

$$\begin{pmatrix} \ddot{F}_1 \\ \ddot{F}_2 \end{pmatrix} = \mathbf{B} \begin{pmatrix} \bar{u}_1 \\ \bar{u}_2 \end{pmatrix}, \tag{11}$$

where

$$\mathbf{B} = \begin{pmatrix} \cos\theta & -v\sin\theta \\ \sin\theta & v\cos\theta \end{pmatrix}. \tag{12}$$

By choosing the inputs $[\bar{u}_1, \bar{u}_2]^T$ as

$$\begin{pmatrix} \bar{u}_1 \\ \bar{u}_2 \end{pmatrix} = \mathbf{B}^{-1}\mathbf{v} = \frac{1}{v}\begin{pmatrix} v\cos\theta & v\sin\theta \\ -\sin\theta & \cos\theta \end{pmatrix}\mathbf{v}, \tag{13}$$

Eq. (11) can be written as

$$\ddot{\mathbf{F}} = \mathbf{v}, \tag{14}$$

where $\mathbf{v}$ is the transformed input that can be used for tracking controller design.

B. Dynamic Model with No Slip

To derive the equations of motion, we use Lagrange's equations (Baruh 1998) expressed as

$$\frac{d}{dt}\left(\frac{\partial T}{\partial \dot{\mathbf{q}}}\right) - \frac{\partial T}{\partial \mathbf{q}} + \mathbf{C}^T\boldsymbol{\lambda} = \mathbf{Q}, \tag{15}$$

where T is the kinetic energy of the system, $\mathbf{Q}$ is the generalized force vector, $\mathbf{C}$ is the coefficient matrix in Eq. (2), and $\boldsymbol{\lambda}$ is the vector of the Lagrange multipliers associated with the constraints. From these, we can obtain the equations of motion (Sarkar et al. 1994) expressed as

$$\mathbf{M}(\mathbf{q})\ddot{\mathbf{q}} + \mathbf{V}(\mathbf{q}, \dot{\mathbf{q}}) = \mathbf{E}(\mathbf{q})\boldsymbol{\tau} - \mathbf{C}^T(\mathbf{q})\boldsymbol{\lambda}, \tag{16}$$

where

$$\mathbf{M} = \begin{pmatrix} m & 0 & 0 \\ 0 & m & 0 \\ 0 & 0 & I_z \end{pmatrix}, \ \mathbf{V} = \mathbf{0}, \tag{17}$$

$$\mathbf{E} = \begin{pmatrix} \cos\theta/r & \cos\theta/r \\ \sin\theta/r & \sin\theta/r \\ b/r & -b/r \end{pmatrix}, \ \boldsymbol{\tau} = \begin{pmatrix} \tau_r \\ \tau_l \end{pmatrix}. \tag{18}$$

Here, m is the mass and I_z the moment of inertia of the robot about its center of mass. r is the radius of the robot's wheels and b half the distance between the two wheels. τ_r and τ_l are the motor torques applied on the robot's right and left wheels, respectively. In this dynamic model, it is assumed that the moments of inertia of the two wheels are negligible compared to that of the mobile robot (Campion et al. 1996; Pathak and Agrawal 2005).

By differentiating Eq. (4), one gets $\ddot{\mathbf{q}} = \dot{\mathbf{S}}\boldsymbol{\nu} + \mathbf{S}\dot{\boldsymbol{\nu}}$. On substituting $\ddot{\mathbf{q}}$ into Eq. (16), premultiplying by $\mathbf{S}^T$, and using the property $\mathbf{C}(\mathbf{q})\mathbf{S}(\mathbf{q}) = \mathbf{0}$, one can finally have

$$\dot{\mathbf{q}} = \mathbf{S}\boldsymbol{\nu}, \tag{19a}$$

$$\dot{\boldsymbol{\nu}} = \mathbf{f}\boldsymbol{\tau}, \tag{19b}$$

where

$$\mathbf{f} = (\mathbf{S}^T\mathbf{M}\mathbf{S})^{-1}\mathbf{S}^T\mathbf{E}. \tag{20}$$

With the input transformation given by

$$\begin{pmatrix} \mu_1 \\ \mu_2 \end{pmatrix} = \mathbf{f}\begin{pmatrix} \tau_r \\ \tau_l \end{pmatrix}, \tag{21}$$

and one prolongation of μ_1, Eq. (19) becomes

$$\begin{aligned} \dot{x} &= v\cos\theta, \\ \dot{y} &= v\sin\theta, \\ \dot{\theta} &= w, \\ \dot{v} &= \mu_1, \\ \dot{\mu}_1 &= \bar{\mu}_1, \\ \dot{w} &= \bar{\mu}_2. \end{aligned} \tag{22}$$

Here, $\bar{\mu}_1$, $\bar{\mu}_2$ are the new inputs for the extended system consisting of six states and satisfy

$$\bar{\mu}_1 = \dot{\mu}_1, \ \bar{u}_2 = \mu_2. \tag{23}$$

It is not difficult to check that all states and inputs can be expressed in terms of the same flat outputs as the kinematic model's, $\mathbf{F} = [x, y]^T$. Similar to the kinematic model, an invertible mapping between the inputs and higher derivatives of the flat outputs can be constructed by differentiating the flat outputs until an input appears. The mapping is given by

$$\begin{pmatrix} \dddot{F}_1 \\ \dddot{F}_2 \end{pmatrix} = \mathbf{A} + \mathbf{B}\begin{pmatrix} \bar{\mu}_1 \\ \bar{\mu}_2 \end{pmatrix}, \tag{24}$$

where

$$\mathbf{A} = \begin{pmatrix} -vw^2\cos\theta - 2w\mu_1\sin\theta \\ -vw^2\sin\theta + 2w\mu_1\cos\theta \end{pmatrix}, \ \mathbf{B} = \begin{pmatrix} \cos\theta & -v\sin\theta \\ \sin\theta & v\cos\theta \end{pmatrix}. \tag{25}$$

Equation (24) can be written as

$$\dddot{\mathbf{F}} = \mathbf{v}, \tag{26}$$

by choosing the inputs $[\bar{\mu}_1, \bar{\mu}_2]^T$ as

$$\begin{pmatrix} \bar{\mu}_1 \\ \bar{\mu}_2 \end{pmatrix} = \mathbf{B}^{-1}\mathbf{v} - \mathbf{A}, \tag{27}$$

where $\mathbf{v}$ is the transformed input that can be used for tracking controller design. It should be noted that the controller has a singularity at $v = 0$, which often exists in nonholonomic systems and precludes stabilization by a smooth time-invariant state feedback (Brockett 1983). However, this singularity can be avoided by reparametrizing the trajectory with a new time scale (Fliess et al. 1995; Sira-Ramirez and Agrawal 2004) or can be dealt with practically as stated in the experiment section (Section VI).

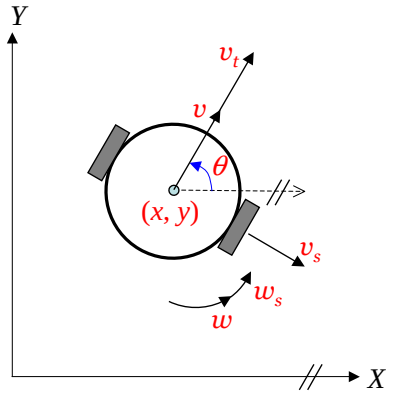

Fig. 2. The velocities of the mobile robot in the presence of slip. v_t and v_s represent the slip velocities in the forward direction and normal to the forward direction, respectively. w_s is the angular slip velocity.

III. Derivation of Slip Model

In this section, we derive the kinematic and dynamic model of the robot with slip of the wheels. It is important to point out that we present a generalized slip model, i.e., the model covers all possible slips of the wheels. The slip is modeled to have component velocities v_t and v_s, as shown in Fig. 2. The robot has another slip component w_s about its vertical axis on the center.

A. Kinematic Model with Slip

With the slip velocity components, the governing equations with slip are given by

$$\begin{aligned} \dot{x} &= (v + v_t)\cos\theta + v_s \sin\theta, \\ \dot{y} &= (v + v_t)\sin\theta - v_s \cos\theta, \\ \dot{\theta} &= w + w_s. \end{aligned} \tag{28}$$

It is valuable to contrast these kinematic equations with slip to the kinematic equations without slip obtained in Eq. (6). Equation (28) reduces to Eq. (6) if $v_t = v_s = w_s = 0$.

Using the input prolongation of v and the input transformation described in Section II-A, the kinematic model with slip is given by

$$\begin{aligned} \dot{x} &= (v + v_t)\cos\theta + v_s \sin\theta, \\ \dot{y} &= (v + v_t)\sin\theta - v_s \cos\theta, \\ \dot{v} &= \bar{u}_1, \\ \dot{\theta} &= \bar{u}_2 + w_s. \end{aligned} \tag{29}$$

B. Dynamic Model with Slip

Considering kinematics with slip velocities as a form of constraints to the motion, one can derive the dynamic equations of motion using the structure of Eq. (16). Using the procedure outlined in Section II-B, the slip dynamic model is given by

$$\dot{\mathbf{q}} = \mathbf{S}\boldsymbol{\nu} + \boldsymbol{\delta}, \tag{30a}$$

$$\dot{\boldsymbol{\nu}} = \mathbf{f}\boldsymbol{\tau} - (\mathbf{S}^T\mathbf{M}\mathbf{S})^{-1}\mathbf{S}^T\mathbf{M}\dot{\boldsymbol{\delta}} \tag{30b}$$

$$= \mathbf{f}\boldsymbol{\tau} - \begin{pmatrix} \cos\theta & \sin\theta & 0 \\ 0 & 0 & 1 \end{pmatrix} \dot{\boldsymbol{\delta}}. \tag{30c}$$

where $\boldsymbol{\delta} = [\delta_1, \delta_2, \delta_3]^T$ and $\delta_1 = v_t\cos\theta + v_s\sin\theta$, $\delta_2 = v_t\sin\theta - v_s\cos\theta$, and $\delta_3 = w_s$. Using the input prolongation of μ_1, similar to Section II-B, Eq. (30), the dynamic model with slip, can be rewritten as

$$\dot{x} = v\cos\theta + v_t\cos\theta + v_s\sin\theta, \tag{31a}$$

$$\dot{y} = v\sin\theta + v_t\sin\theta - v_s\cos\theta, \tag{31b}$$

$$\dot{\theta} = w + w_s, \tag{31c}$$

$$\dot{v} = \mu_1 - \dot{v}_t - v_s\dot{\theta}, \tag{31d}$$

$$\dot{\mu}_1 = \bar{\mu}_1, \tag{31e}$$

$$\dot{w} = \bar{\mu}_2 - \dot{w}_s. \tag{31f}$$

IV. Design of Control Law

A. Based on Kinematic Model with Slip

For the kinematic slip model described in Eq. (29), similar to Section II-A, one can write the following relationship

$$\begin{pmatrix} \ddot{F}_1 \\ \ddot{F}_2 \end{pmatrix} = \mathbf{B}\begin{pmatrix} \bar{u}_1 \\ \bar{u}_2 \end{pmatrix} + \left\{ \mathbf{C} + \mathbf{D}\begin{pmatrix} \bar{u}_1 \\ \bar{u}_2 \end{pmatrix} \right\}, \tag{32}$$

where the matrix $\mathbf{B}$ is the same as the one in the no-slip model given in Eq. (11). The matrices $\mathbf{C}$ and $\mathbf{D}$ are functions of the slip velocity components as well as the states of the system and are given by

$$\mathbf{C} = \begin{pmatrix} (v_s w_s + \dot{v}_t)\cos\theta - (v w_s + v_t w_s - \dot{v}_s)\sin\theta \\ (v_s w_s + \dot{v}_t)\sin\theta + (v w_s + v_t w_s - \dot{v}_s)\cos\theta \end{pmatrix}, \tag{33}$$

$$\mathbf{D} = \begin{pmatrix} 0 & -v_t\sin\theta + v_s\cos\theta \\ 0 & v_t\cos\theta + v_s\sin\theta \end{pmatrix}. \tag{34}$$

These matrices become zero when $v_t(t) = v_s(t) = w_s(t) = 0$. Therefore, Eq. (32) simplifies to Eq. (11) in the absence of slip. The slip velocity components can be thought of as disturbances into the system because their time histories are unknown. Hence, by choosing the same form of the inputs as in Eq. (13), we can represent this system as two linear double integrator plants with uncertainty given by

$$\ddot{\mathbf{F}} = \mathbf{v} + \boldsymbol{\eta}, \tag{35}$$

where

$$\boldsymbol{\eta} = \mathbf{D}\mathbf{B}^{-1}\mathbf{v} + \mathbf{C} \tag{36}$$

$$\equiv \mathbf{E}\mathbf{v} + \mathbf{G}. \tag{37}$$

Note that the uncertainty $\boldsymbol{\eta}$ is a 2-dimensional vector and depends on the slip velocity components, the evolution of the states, and the inputs to the system.

Let us define (2×1) error vectors such that

$$\mathbf{e_1} = \mathbf{F} - \mathbf{F_d}, \tag{38}$$

$$\mathbf{e_2} = \dot{\mathbf{F}} - \dot{\mathbf{F}}_\mathbf{d}. \tag{39}$$

Here, $\mathbf{F_d}(t)$ being a feasible reference trajectory achievable by the no-slip model. The computation of such a feasible reference trajectory will come from the differentially flat representation of the no-slip model. By introducing $\mathbf{e} = [\mathbf{e_1}, \mathbf{e_2}]^T$, one gets the following state space forms

$$\dot{\mathbf{e}} = \mathbf{H}\mathbf{e} + \mathbf{J}(\mathbf{v} + \boldsymbol{\eta} - \ddot{\mathbf{F}}_\mathbf{d}), \tag{40}$$

where

$$\mathbf{H} = \begin{pmatrix} \mathbf{0} & \mathbf{I} \\ \mathbf{0} & \mathbf{0} \end{pmatrix}, \ \mathbf{J} = \begin{pmatrix} \mathbf{0} \\ \mathbf{I} \end{pmatrix}, \tag{41}$$

and $\mathbf{I}$ denotes the (2×2) identity matrix.

We adopted the following structure of the control law from Spong and Vidyasagar (1989) to track the reference trajectory $\mathbf{F_d}(t)$

$$\mathbf{v} = \hat{\mathbf{v}} + \Delta\mathbf{v}, \tag{42}$$

where $\hat{\mathbf{v}}$ represents the nominal stabilizing control for the no-slip model utilizing the differentially flat double integrator model outlined in Section II-A. The structure of $\hat{\mathbf{v}}$ is given by

$$\begin{aligned} \hat{\mathbf{v}} &= \ddot{\mathbf{F}}_\mathbf{d} - \mathbf{K_1 e_1} - \mathbf{K_2 e_2} \\ &\equiv \ddot{\mathbf{F}}_\mathbf{d} - \mathbf{K e}, \end{aligned} \tag{43}$$

where $\mathbf{K} = [\mathbf{K_1} \ \mathbf{K_2}]$ and $\mathbf{K_i}$, $i = 1, 2$, is a (2×2) diagonal matrix of control gains that make the closed-loop nominal system exponentially stable when there is no slip. The additional corrective control term $\Delta\mathbf{v}$ is now chosen to overcome the effects of the uncertainty $\boldsymbol{\eta}$.

On substituting the control law given by Eq. (42), with the nominal control $\hat{\mathbf{v}}$ given in Eq. (43), into Eq. (40), the error dynamics turns into the following form:

$$\dot{\mathbf{e}} = \bar{\mathbf{A}}\mathbf{e} + \mathbf{J}\{\Delta\mathbf{v} + \boldsymbol{\eta}\}, \tag{44}$$

where $\bar{\mathbf{A}} = \mathbf{H} - \mathbf{JK}$ and it is Hurwitz.

We make the following assumptions about the slip velocities and their derivatives.

Assumption 4.1: The slip velocities v_t and v_s are bounded and possess the property

$$\|v_t\| + \|v_s\| \leq 2\alpha\|v\|, \text{ where } 0 \leq \alpha < 0.5. \tag{45}$$

Note that this assumption is reasonable. Physically, this means that the magnitude of the slip component v_t plus the magnitude of the slip component v_s is smaller than the magnitude of the vehicle's forward velocity. From an engineering perspective, we expect the slip velocity to be small compared to the speed of the vehicle.

Assumption 4.2: $\|w_s\|$, $\|\dot{v}_t\|$, and $\|\dot{v}_s\|$ are bounded such that

$$\|w_s\| \leq \zeta_1, \quad \|\dot{v}_t\| \leq \zeta_2, \quad \|\dot{v}_s\| \leq \zeta_3. \tag{46}$$

where ζ_i, $i = 1, ..., 3$, is a known value or function of the state variables.

Under these assumptions, the corrective control term $\Delta\mathbf{v}$ can be made according to the following theorem:

Theorem 4.3: The system presented by Eq. (44) is globally asymptotically stable using the control structure of Eq. (42) if the nominal control $\hat{\mathbf{v}}$ is given by Eq. (43) and the corrective term $\Delta\mathbf{v}$ is chosen in the following way:

$$\Delta\mathbf{v} = \begin{cases} -\rho(\mathbf{e}, t)\frac{\mathbf{J}^T\mathbf{P}\mathbf{e}}{\|\mathbf{J}^T\mathbf{P}\mathbf{e}\|} & \text{for } \|\mathbf{J}^T\mathbf{P}\mathbf{e}\| \neq 0 \\ 0 & \text{for } \|\mathbf{J}^T\mathbf{P}\mathbf{e}\| = 0 \end{cases}, \tag{47}$$

where (i) ϵ is a small positive number, (ii) $\mathbf{P}$ is the unique positive definite symmetric solution of the Lyapunov equation

$$\bar{\mathbf{A}}^T\mathbf{P} + \mathbf{P}\bar{\mathbf{A}} + \mathbf{Q} = \mathbf{0}, \tag{48}$$

with $\mathbf{Q}$ as a symmetric positive definite matrix, and (iii) $\|\Delta\mathbf{v}\| \leq \rho$, $\|\boldsymbol{\eta}\| \leq \rho$.

Proof: First, one can show, through simple algebra, that

$$\|\mathbf{E}\| = \|\mathbf{D}\mathbf{B}^{-1}\| = \sqrt{\lambda_{max}(\mathbf{E}^T\mathbf{E})} \tag{49}$$

$$= \frac{\sqrt{v_t^2 + v_s^2}}{\|v\|} \tag{50}$$

$$\leq \frac{\|v_t\| + \|v_s\|}{\|v\|}. \tag{51}$$

From Assumption 4.1, $\|\mathbf{E}\|$ satisfies the following property

$$\|\mathbf{E}\| \leq 2\alpha < 1. \tag{52}$$

Since $\mathbf{G}$ is a function of the slip velocities and their derivatives as well as the state variables, on exploring the structure of individual terms that constitute $\mathbf{G}$ using Assumptions 4.1 and 4.2, it is possible to find a function Φ of the state variables and known values such that

$$\|\mathbf{G}\| \leq \Phi. \tag{53}$$

With these properties, one can obtain ρ which is defined implicitly below.

$$\|\boldsymbol{\eta}\| = \|\mathbf{E}\mathbf{v} + \mathbf{G}\| \tag{54}$$

$$\leq \|\mathbf{E}\|\|\hat{\mathbf{v}}\| + \|\mathbf{E}\|\|\Delta\mathbf{v}\| + \|\mathbf{G}\| \tag{55}$$

$$\leq 2\alpha\|\hat{\mathbf{v}}\| + 2\alpha\rho + \Phi \tag{56}$$

$$:= \rho. \tag{57}$$

Therefore, ρ is obtained as

$$\rho = \frac{1}{1 - 2\alpha}\left(2\alpha\|\hat{\mathbf{v}}\| + \Phi\right). \tag{58}$$

Using a Lyapunov candidate $V = \mathbf{e}^T\mathbf{P}\mathbf{e}$, it can be proven $\dot{V} < 0$ by following the steps in the proof given in Appendix. ■

However, this control law causes chattering in its control signal, which is a common characteristic of discontinuous control. To avoid the chattering, we introduce the following continuous control which will be used for the simulation study in the next section.

Theorem 4.4: The system presented by Eq. (44) is uniformly ultimately bounded using the control structure of Eq. (42) if the nominal control $\hat{\mathbf{v}}$ is given by Eq. (43) and the corrective term $\Delta\mathbf{v}$ is chosen in the following way:

$$\Delta\mathbf{v} = \begin{cases} -\rho(\mathbf{e}, t)\frac{\mathbf{J}^T\mathbf{P}\mathbf{e}}{\|\mathbf{J}^T\mathbf{P}\mathbf{e}\|} & \text{for } \|\mathbf{J}^T\mathbf{P}\mathbf{e}\| \geq \epsilon \\ -\rho(\mathbf{e}, t)\frac{\mathbf{J}^T\mathbf{P}\mathbf{e}}{\epsilon} & \text{for } \|\mathbf{J}^T\mathbf{P}\mathbf{e}\| < \epsilon \end{cases}, \tag{59}$$

where (i) ϵ is a small positive number, (ii) $\mathbf{P}$ is the unique positive definite symmetric solution of the Lyapunov equation

$$\bar{\mathbf{A}}^T\mathbf{P} + \mathbf{P}\bar{\mathbf{A}} + \mathbf{Q} = \mathbf{0}, \tag{60}$$

with $\mathbf{Q}$ as a symmetric positive definite matrix, and (iii) $\|\Delta\mathbf{v}\| \leq \rho$, $\|\boldsymbol{\eta}\| \leq \rho$.
The proof of this theorem is provided in Appendix.

B. Based on Dynamic Model with Slip

For the dynamic slip model described in Eq. (31), similar to Section II-B, one can write the following relationship

$$\begin{pmatrix} \dddot{F}_1 \\ \dddot{F}_2 \end{pmatrix} = \mathbf{A} + \mathbf{B}\begin{pmatrix} \bar{\mu}_1 \\ \bar{\mu}_2 \end{pmatrix} + \left\{ \mathbf{C} + \mathbf{D}\begin{pmatrix} \bar{\mu}_1 \\ \bar{\mu}_2 \end{pmatrix} \right\}, \tag{61}$$

where the matrices $\mathbf{A}$ and $\mathbf{B}$ are the same as the no-slip model's given in Eq. (25) and

$$\mathbf{C} = \begin{pmatrix} (\dot{v}_s w - v_t w^2)\cos\theta + (v_s w^2 + v\dot{w}_s + v_t\dot{w}_s + \ddot{v}_s)\sin\theta \\ (\dot{v}_s w - v_t w^2)\sin\theta - (v_s w^2 + v\dot{w}_s + v_t\dot{w}_s + \ddot{v}_s)\cos\theta \end{pmatrix},$$

$$\mathbf{D} = \begin{pmatrix} 0 & -v_t\sin\theta \\ 0 & v_t\cos\theta \end{pmatrix}.$$

These matrices also become zero, simplifying Eq. (61) to Eq. (24), when $v_t(t) = v_s(t) = w_s(t) = 0$.

Hence, we can represent this system as two linear triple integrator plants with uncertainty given by

$$\dddot{\mathbf{F}} = \mathbf{v} + \boldsymbol{\eta}, \tag{62}$$

where

$$\boldsymbol{\eta} = \mathbf{D}\mathbf{B}^{-1}\mathbf{v} + (\mathbf{C} - \mathbf{D}\mathbf{B}^{-1}\mathbf{A}) \tag{63}$$

$$\equiv \mathbf{E}\mathbf{v} + \mathbf{G} \tag{64}$$

By introducing $\mathbf{e} = [\mathbf{e_1}, \mathbf{e_2}, \mathbf{e_3}]^T$ with $\mathbf{e_1} = \mathbf{F} - \mathbf{F_d}$, $\mathbf{e_2} = \dot{\mathbf{F}} - \dot{\mathbf{F}}_\mathbf{d}$, and $\mathbf{e_3} = \ddot{\mathbf{F}} - \ddot{\mathbf{F}}_\mathbf{d}$, one can get the following state space forms.

$$\dot{\mathbf{e}} = \mathbf{H}\mathbf{e} + \mathbf{J}(\mathbf{v} + \boldsymbol{\eta} - \dddot{\mathbf{F}}_\mathbf{d}), \tag{65}$$

where

$$\mathbf{H} = \begin{pmatrix} \mathbf{0} & \mathbf{I} & \mathbf{0} \\ \mathbf{0} & \mathbf{0} & \mathbf{I} \\ \mathbf{0} & \mathbf{0} & \mathbf{0} \end{pmatrix}, \mathbf{J} = \begin{pmatrix} \mathbf{0} \\ \mathbf{0} \\ \mathbf{I} \end{pmatrix}, \tag{66}$$

and $\mathbf{I}$ denotes the (2×2) identity matrix.

Similar to the previous section, the structure of the control law takes the form of

$$\mathbf{v} = \hat{\mathbf{v}} + \Delta\mathbf{v}, \tag{67}$$

with $\hat{\mathbf{v}}$ given by

$$\hat{\mathbf{v}} = \ddot{\mathbf{F}}_\mathbf{d} - \mathbf{K_1}\mathbf{e_1} - \mathbf{K_2}\mathbf{e_2} - \mathbf{K_3}\mathbf{e_3}$$

$$\equiv \dddot{\mathbf{F}}_\mathbf{d} - \mathbf{K}\mathbf{e}, \tag{68}$$

where $\mathbf{K} = [\mathbf{K_1}\ \mathbf{K_2}\ \mathbf{K_3}]$ and $\mathbf{K_i}$, $i = 1, 2, 3$, is a (2×2) diagonal matrix of control gains for the nominal system.

On substituting the control law given by Eq. (67), with the nominal control $\hat{\mathbf{v}}$ given in Eq. (68), into Eq. (65), the error dynamics takes the following form:

$$\dot{\mathbf{e}} = \bar{\mathbf{A}}\mathbf{e} + \mathbf{J}\{\Delta\mathbf{v} + \boldsymbol{\eta}\}, \tag{69}$$

where $\bar{\mathbf{A}} = \mathbf{H} - \mathbf{J}\mathbf{K}$ and it is Hurwitz.

We make the following assumptions about the slip velocities and their derivatives.

Assumption 4.5: The slip velocity v_t is bounded and possess the property

$$\|v_t\| \leq \alpha\|v\|, \text{ where } 0 \leq \alpha < 1 \tag{70}$$

Assumption 4.6: $\|w_s\|$, $\|v_s\|$, $\|\dot{v}_s\|$, and $\|\ddot{v}_s\|$ are bounded such that

$$\|w_s\| \leq \xi_1. \quad \|v_s\| \leq \xi_2, \tag{71}$$

$$\|\dot{v}_s\| \leq \xi_3, \quad \|\ddot{v}_s\| \leq \xi_4, \tag{72}$$

where ξ_i, $i = 1, ..., 4$, is a known value or function of the state variables.
Under these assumptions, similar to the kinematic model case, the corrective control term $\Delta\mathbf{v}$ can be made according to the following theorem:

Theorem 4.7: The system presented by Eq. (69) is uniformly ultimately bounded using the control structure of Eq. (67) if the nominal control $\hat{\mathbf{v}}$ is given by Eq. (68) and the corrective term $\Delta\mathbf{v}$ is chosen in the following way:

$$\Delta\mathbf{v} = \begin{cases} -\rho(\mathbf{e}, t)\frac{\mathbf{J}^T\mathbf{P}\mathbf{e}}{\|\mathbf{J}^T\mathbf{P}\mathbf{e}\|} & \text{for } \|\mathbf{J}^T\mathbf{P}\mathbf{e}\| \geq \epsilon \\ -\rho(\mathbf{e}, t)\frac{\mathbf{J}^T\mathbf{P}\mathbf{e}}{\epsilon} & \text{for } \|\mathbf{J}^T\mathbf{P}\mathbf{e}\| < \epsilon \end{cases}, \tag{73}$$

where (i) ϵ is a small positive number, (ii) $\mathbf{P}$ is the unique positive definite symmetric solution of the Lyapunov equation

$$\bar{\mathbf{A}}^T\mathbf{P} + \mathbf{P}\bar{\mathbf{A}} + \mathbf{Q} = \mathbf{0}, \tag{74}$$

with $\mathbf{Q}$ as a symmetric positive definite matrix, and (iii) $\|\Delta\mathbf{v}\| \leq \rho$, $\|\boldsymbol{\eta}\| \leq \rho$.

Proof: First, through simple algebra, one can show that

$$\|\mathbf{E}\| = \|\mathbf{D}\mathbf{B}^{-1}\| = \sqrt{\lambda_{max}(\mathbf{E}^T\mathbf{E})}$$

$$= \frac{\|v_t\|}{\|v\|}. \tag{75}$$

From Assumption 4.5, $\|\mathbf{E}\|$ satisfies the following property

$$\|\mathbf{E}\| \leq \alpha < 1. \tag{76}$$

On exploring the structure of individual terms that constitute $\|\mathbf{G}\|$ and using Assumptions 4.5 and 4.6, it is possible to find Φ such that

$$\|\mathbf{G}\| \leq \Phi. \tag{77}$$

TABLE I
END CONDITIONS USED IN PLANNING

t_i = 0	$x = 0$	$y = 0$	$\theta = \frac{\pi}{2}$	$v = 0.15$
t_f = 20	$x = 1.2$	$y = 1.5$	$\theta = \frac{\pi}{2}$	$v = 0.15$

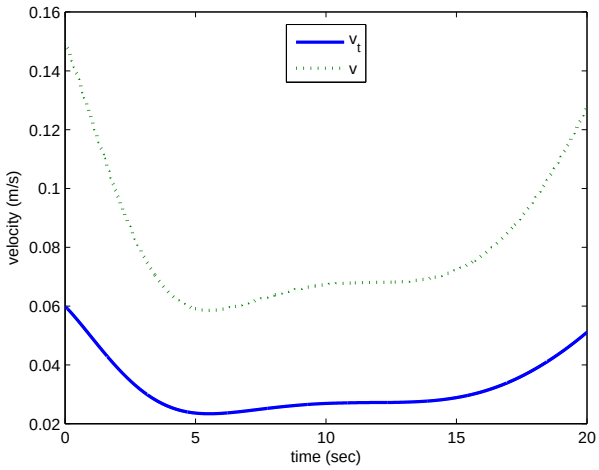

Fig. 3. The slip velocity $v_t(t)$ used in the robust kinematic controller simulation. The magnitude of $v_t(t)$ is 40 % of that of $v(t)$.

With these properties, one can obtain ρ which is defined implicitly below.

$$\|\boldsymbol{\eta}\| = \|\mathbf{E}\mathbf{v} + \mathbf{G}\| \tag{78}$$
$$\leq \alpha\|\hat{\mathbf{v}}\| + \alpha\rho + \Phi \tag{79}$$
$$:= \rho. \tag{80}$$

Therefore, ρ is obtained as

$$\rho = \frac{1}{1-\alpha}\left(\alpha\|\hat{\mathbf{v}}\| + \Phi\right). \tag{81}$$

With a Lyapunov candidate $V = \mathbf{e}^T P \mathbf{e}$, the rest of this proof also follows the proof of Theorem 4.4 given in Appendix. ■

V. SIMULATION RESULTS

Desired trajectories for point-to-point motion of the system were planned using the differential parameterization constructed in Section II. The desired trajectories were individually generated based on the no-slip kinematic model in Eq. (7) and the no-slip dynamic model in Eq. (22). For illustration, polynomials were taken for the desired trajectories of the flat outputs ($F_1(t)$, $F_2(t)$) = ($x(t)$,$y(t)$) over t = [0, 20] sec by determining the coefficients of polynomials using the corresponding end conditions in flat output space. The end conditions of the original states, used in planning, are listed in Table I. For the trajectory of the dynamic controller, the following conditions were additionally used: $w(0) = w(t_f) = 0$, $\mu_1(0) = \mu_1(t_f) = 0$. All units are in SI and angles in radians.

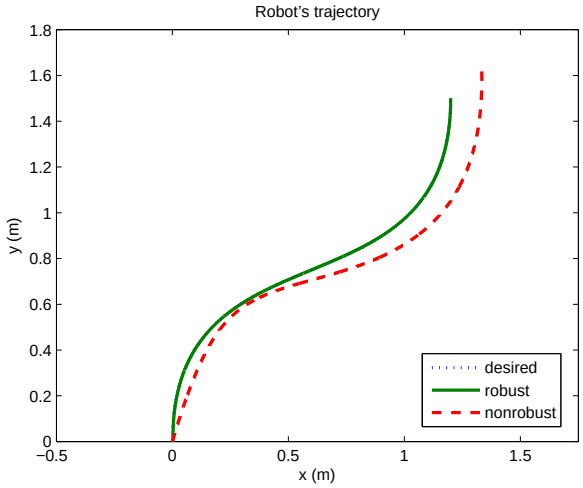

Fig. 4. The simulation results of the kinematic controller for the mobile robot. The desired trajectory is generated using the no-slip kinematic model. The actual trajectories are simulated under the robust control and the nominal(nonrobust) control.

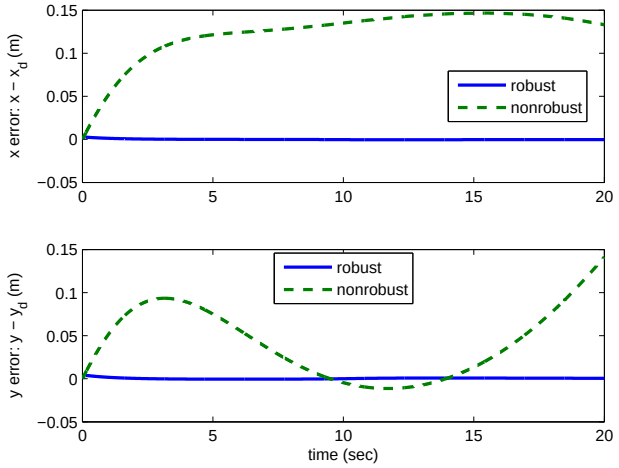

Fig. 5. The tracking errors for $x(t)$, $y(t)$ under the robust control and the nonrobust control with the slip-kinematic model.

A. Robust Kinematic Controller

Using the slip model Eq. (29) for simulation, we assumed that slip velocities of v_t and v_s are bounded as follows

$$\|v_t\| \leq \alpha\|v\|, \quad \|v_s\| \leq \alpha\|v\|, \tag{82}$$

so that Assumption 4.1 is valid. We chose $\alpha = 0.4$, i.e., the slip velocities v_t, v_s can be up to 40 % of the forward speed. In order to check the controller performance in harsher conditions, we assumed that the slip velocities are at their upper bound at all times, i.e.,

$$v_t(t) = \alpha v(t), \quad v_s(t) = \alpha v(t). \tag{83}$$

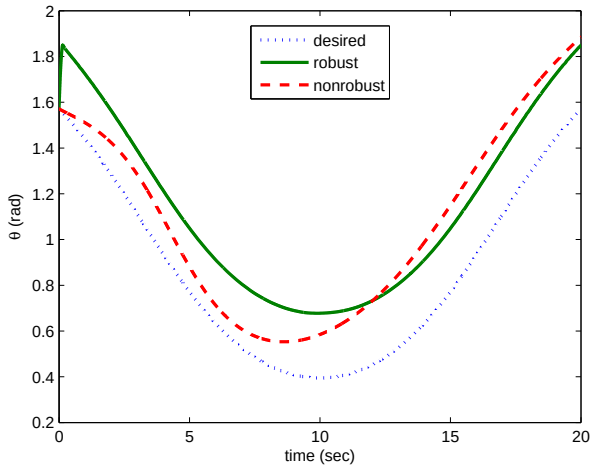

Fig. 6. The desired and actual trajectories of θ with the slip-kinematic model.

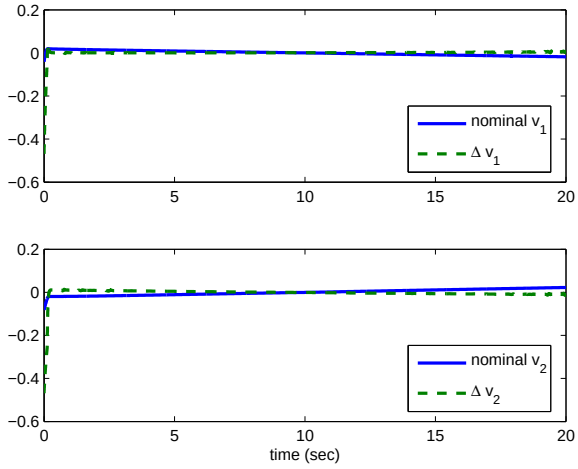

Fig. 7. The nominal control term $\hat{\mathbf{v}}$ given in Eq. (43) and corrective control term $\Delta\mathbf{v}$ in Eq. (47) of the robust kinematic controller.

Using a similar reasoning, the angular slip velocity w_s was also assumed to be

$$w_s(t) = \alpha v(t). \tag{84}$$

These slip velocities are consistent with the following bound of the other unknown values: $\|\dot{v}_t\| \leq \alpha\|\hat{v}_1\|$ and $\|\dot{v}_s\| \leq \alpha\|\hat{v}_1\|$. In addition, ϵ in Eq. (47) was chosen to be 0.02. The control gains $\mathbf{K}_i$ for the nominal control in Eq. (43) were selected so that all the roots of the characteristic equations of the error dynamics for the no-slip model are at -0.5. The values are $\mathbf{K_1} = diag\{0.25, 0.25\}$ and $\mathbf{K_2} = diag\{1, 1\}$. Consequently, the Lyapunov equation in Eq. (48) can be solved with $\mathbf{Q}$ being a (4×4) identity matrix.

The time history of the slip velocity $v_t(t)$, defined as in Eq. (83), is shown in Fig. 3. As defined, the magnitude of $v_t(t)$ is 40 % of $v(t)$. The same value of $v_t(t)$ is used for the other slip velocities $v_s(t)$ and $w_s(t)$ in the simulation as we assumed in Eqs. (83) and (84).

Figure 4 shows the desired and actual trajectories under two forms of control: (i) robust control with $\Delta\mathbf{v}$ added in, (ii) nominal control without $\Delta\mathbf{v}$. The robust controller makes the robot more accurately track the desired trajectory while rejecting the slip disturbance, whereas the nominal controller presents significant errors during motion. As shown in Fig. 5, the tracking error with the robust control is much smaller (nearly zero) compared to the nominal control in the presence of slip. Note that the use of higher gains for $\mathbf{K}_i$ in the nonrobust control could reduce the tracking error, however, one cannot guarantee the uniformly ultimate boundedness property of the robust controller.

In Fig. 6, the desired and the actual trajectories for θ are shown. Once the desired trajectories for the flat outputs (x, y) are planned, the desired trajectories for another state variable θ can be easily calculated using the diffeomorphism constructed in Section II-A. As shown in the figure, the actual trajectory of θ does not follow exactly the no-slip based desired trajectory not only with the nonrobust controller but also with the robust controller. This is also consistent with the fact that in the presence of slip, the mobile robot is not constrained to be oriented to the tangent to the path. The deviation from the desired trajectory is because in the design of the robust controller, the uniform ultimate boundedness is only guaranteed for x and y.

Figure 7 shows the nominal control input $\hat{\mathbf{v}}$ and the corrective control term $\Delta\mathbf{v}$ of the robust controller. ϵ in Eq. (47) was chosen to be 0.02 for the simulation, which was the smallest value in order to reasonably avoid chattering in the control under the given conditions.

B. Robust Dynamic Controller

Using the slip model in Eq. (31) for simulation, we assumed that the slip velocity v_t is bounded in a way that

$$\|v_t\| \leq \alpha\|v\|, \tag{85}$$

so that Assumption 4.5 is valid. We chose $\alpha = 0.3$ and assumed that the slip velocity is at their upper bound at all times, i.e.,

$$v_t(t) = \alpha v(t). \tag{86}$$

Using a similar reasoning, the other slip velocities of v_s, w_s were also assumed to be

$$v_s(t) = \alpha v(t), \tag{87}$$

$$w_s(t) = \alpha v(t). \tag{88}$$

In addition, ϵ in Eq. (73) was chosen to be 0.005. The control gains $\mathbf{K}_i$ for the nominal control in Eq. (68) were selected so that all the roots of the characteristic equations of the error dynamics for the no-slip model are at -0.5. The values are $\mathbf{K_1} = diag\{0.125, 0.125\}$, $\mathbf{K_2} = diag\{0.75, 0.75\}$, and $\mathbf{K_3} = diag\{1.5, 1.5\}$. Consequently, the Lyapunov equation in Eq. (48) can be solved with $\mathbf{Q}$ being a (6×6) identity matrix.

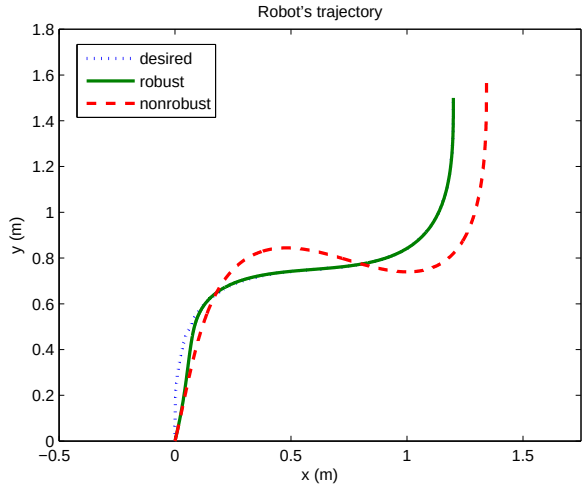

Fig. 8. The simulation results of the dynamic controller under the robust control and the nonrobust control.

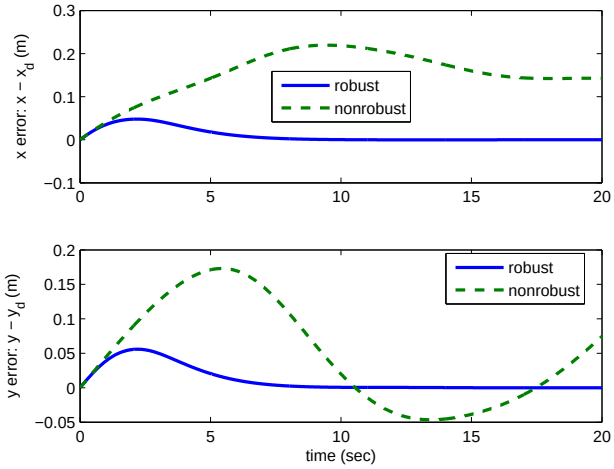

Fig. 9. The tracking errors for $x(t)$, $y(t)$ under the robust control and the nonrobust control with the slip-dynamic model.

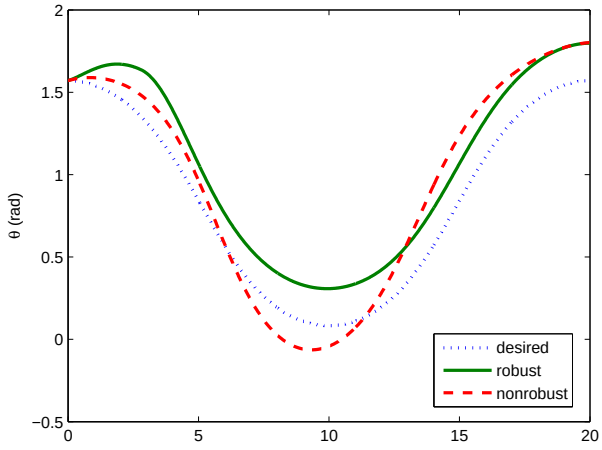

Fig. 10. The desired and actual trajectories of θ with the slip-dynamic model.

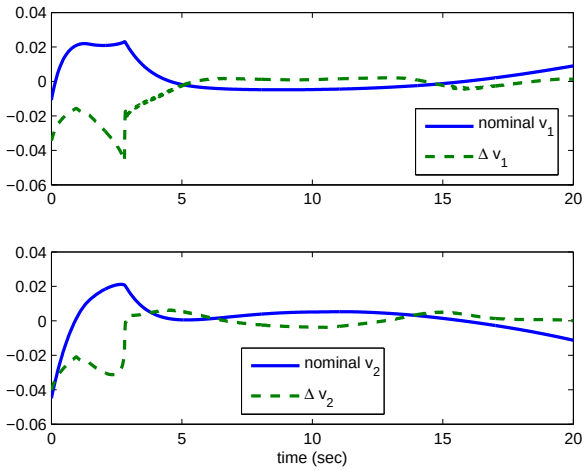

Fig. 11. The nominal control term $\hat{\mathbf{v}}$ and corrective control term $\Delta\mathbf{v}$ (given in Eq. (73)) in Eq. (68) of the robust dynamic controller.

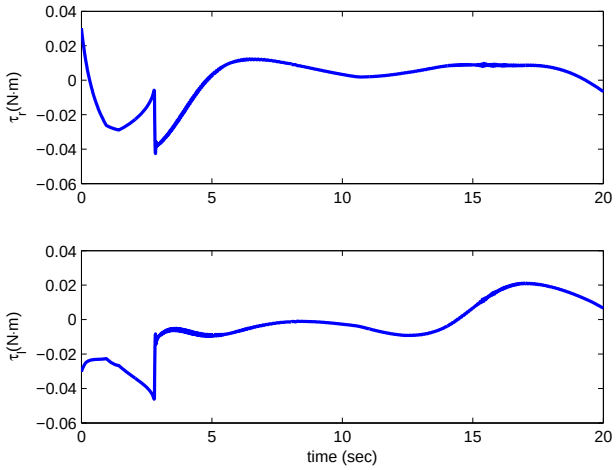

Fig. 12. The computed original torque inputs with the robust dynamic controller. τ_r is the torque for the robot's right wheel and τ_r for the left wheel, respectively.

TABLE II
SYSTEM PARAMETER VALUES

m	18.2 kg	mass of the robot
I_z	0.39375 kg·m^2	moment of inertia
r	0.0825 m	wheel radius
b	0.1624 m	half distance between the wheels

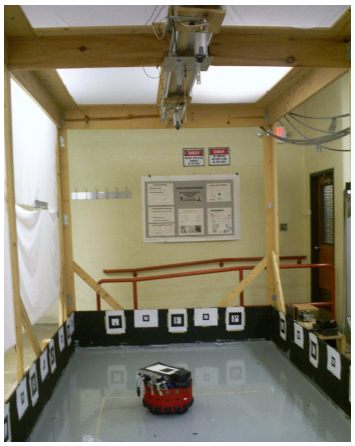

Fig. 13. Experimental setup using an overhead camera which detects the pattern placed on the top of the robot and gives the position and orientation data of the mobile robot.

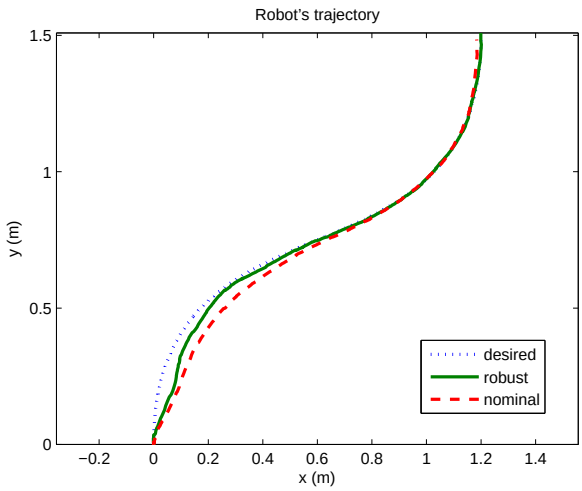

Fig. 14. Experimental results for the mobile robot.

Figure 8 shows the desired and actual trajectories under robust control and nominal control. The robust controller makes the robot recover more quickly from the error at the beginning, which resulted from the slip disturbances, and track the desired trajectory with smaller error. As shown in Fig. 9, the tracking error with the robust control is much smaller compared to the nominal control with slip. In Fig. 10, the desired and the actual trajectory for θ is shown. Figure 11 shows the nominal control input $\hat{\mathbf{v}}$ and the corrective control term $\Delta\mathbf{v}$ of the robust controller.

By substituting Eq. (67) into Eq. (27), one can obtain the control inputs $\bar{\mu}_1$ and $\bar{\mu}_2$ for the prolonged system. Then, the original control inputs τ_r, τ_l can be computed using Eq. (23) and by integration. The system parameters used in the simulations to calculate the original torques are listed in Table II and are the real values of iRobot's Magellan Pro mobile robot used in the experiment in the next section.

VI. Experimental Results of the Kinematic Controller

To validate the proposed controller, experiments were conducted by implementing the control algorithm on iRobot's Magellan Pro mobile robot. As shown in Fig. 13, the laboratory setup has a calibrated overhead camera for providing absolute position and orientation data by detecting the pattern on top of the robot. The position and orientation data was used to correct the robot's own odometry drift at about 3 Hz. Since the Magellan Pro programming interface allows only forward speed v and turning speed w to be set as command inputs, the kinematic controller was used for the experiments.

We used the same desired trajectory as the one used in the simulation presented in Section V-A. However, in this experiment's controller design, we assumed that the slip velocities will not be high due to the flat and clean surface of the test area in the laboratory and relatively low speed during motion. Therefore, we set α in Eq. (45) as 0.1. ϵ is an important factor to reduce chattering in control. Through simulation and experimental iteration, we found an appropriate value for ϵ to be 0.1 for the control.

Figure 14 shows the desired and actual trajectories under robust control and nominal control. Note that there are relatively large errors at the beginning of the motion for both nominal and robust controllers. As mentioned in the previous section, these controllers have a singularity at $v = 0$. To avoid the singularity problem in practice, especially when a mobile robot starts at rest, we used the robot's forward speed v to be 0.05 (m/s) whenever it went below 0.05 (m/s). The error in the experimental results at the beginning of the motion comes from this fact that we planned the desired trajectory assuming that the robot starts with v = 0.15 (m/s), even though the robot is starting at zero speed. Despite the errors, the robust controller makes the robot track the desired trajectory better, whereas the nominal controller presents larger errors during motion.

As shown in Fig. 15, the tracking error with the robust control is smaller compared to the nominal control with slip. Some fluctuation in the error of nonrobust control is shown as a consequence of the fluctuation in control input in Fig. 16 as is expected in this type of robust control. However, it is observed that between approximately 15 and 20 seconds, the robust control has larger errors in y than the nonrobust control. This may be because the effect of slippage might not have been significant due to the relatively low speeds and the nonslippery surface. Figure 16 shows the nominal control input $\hat{\mathbf{v}}$ and the corrective control term $\Delta\mathbf{v}$ for the robust controller.

VII. Conclusions

In this paper, robust trajectory-tracking controllers for differentially driven two-wheeled mobile robots are proposed based on (i) the kinematic model with slip and (ii) the dynamic model with slip, respectively. The controllers were developed by extending the framework of the differential flatness theory to the models with slip uncertainties. The simulation and experiment results show that the proposed robust controllers are effective

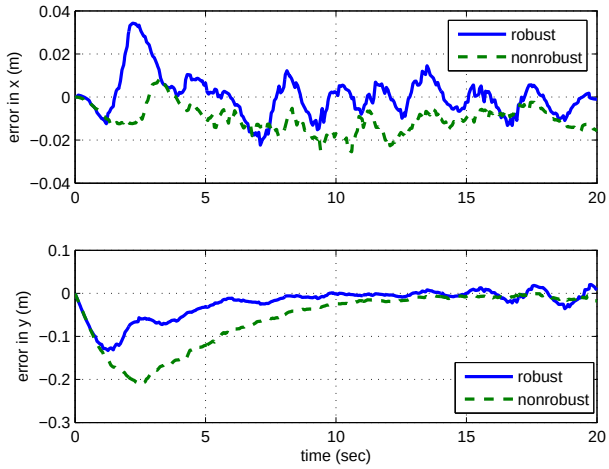

Fig. 15. The tracking errors for $x(t)$, $y(t)$ with the kinematic robust and nominal control.

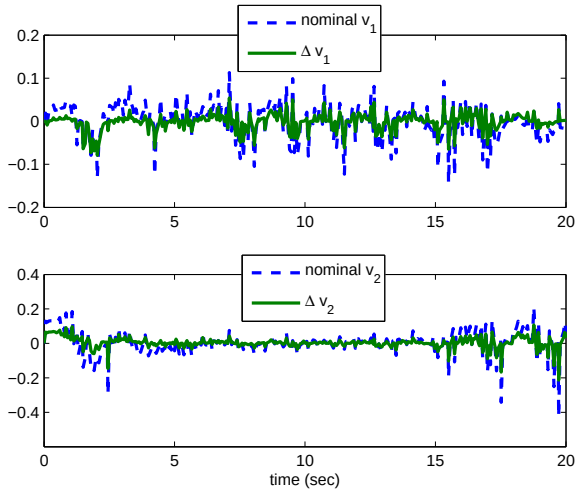

Fig. 16. The nominal control term $\hat{\mathbf{v}}$ given in Eq. (68) and corrective control term $\Delta\mathbf{v}$ in Eq. (73) with the kinematic robust control in the experiment.

in the presence of slip. Moreover, differential flatness presents a valuable framework for integrated planning and control of mobile robots in the presence of slip. Future work will include experiments with the dynamic controller and development of an improved controller with explicit consideration of modeling uncertainties.

APPENDIX

Proof of Theorem 4.3 (from Spong and Vidyasagar (1989)): Using a Lyapunov candidate $V = \mathbf{e}^T\mathbf{P}\mathbf{e}$,

$$\dot{V} = \dot{\mathbf{e}}^T\mathbf{P}\mathbf{e} + \mathbf{e}^T\mathbf{P}\dot{\mathbf{e}} \tag{89}$$

$$= \mathbf{e}^T(\bar{\mathbf{A}}^T\mathbf{P} + \mathbf{P}\bar{\mathbf{A}})\mathbf{e} + 2\mathbf{e}^T\mathbf{P}\mathbf{J}(\Delta\mathbf{v} + \boldsymbol{\eta}) \tag{90}$$

$$= -\mathbf{e}^T\mathbf{Q}\mathbf{e} + 2\mathbf{w}^T(\Delta\mathbf{v} + \boldsymbol{\eta}). \tag{91}$$

where $\mathbf{w}$ is set as $\mathbf{J}^T\mathbf{P}\mathbf{e}$ for simplicity.

When $\mathbf{w} = \mathbf{0}$, obviously, $\dot{V} = -\mathbf{e}^T\mathbf{Q}\mathbf{e} < 0$.

When $\mathbf{w} \neq \mathbf{0}$, the half of the second term in Eq. (91) turns out

$$\begin{aligned}\mathbf{w}^T\left(-\rho\frac{\mathbf{w}}{\|\mathbf{w}\|} + \boldsymbol{\eta}\right) &= -\rho\frac{\mathbf{w}^T\mathbf{w}}{\|\mathbf{w}\|} + \mathbf{w}^T\boldsymbol{\eta} \\ &\leq -\rho\|\mathbf{w}\| + \|\mathbf{w}\|\|\boldsymbol{\eta}\| \\ &= \|\mathbf{w}\|(-\rho + \|\boldsymbol{\eta}\|) \\ &\leq 0,\end{aligned} \tag{92}$$

since $\|\boldsymbol{\eta}\| \leq \rho$. Therefore, $\dot{V} < 0$. ■

Proof of Theorem 4.4 (from Spong and Vidyasagar (1989)): Using the Lyapunov candidate $V = \mathbf{e}^T\mathbf{P}\mathbf{e}$ with $\mathbf{w}$ denoting $\mathbf{J}^T\mathbf{P}\mathbf{e}$ as before, one gets

$$\dot{V} = -\mathbf{e}^T\mathbf{Q}\mathbf{e} + 2\mathbf{w}^T(\Delta\mathbf{v} + \boldsymbol{\eta}). \tag{93}$$

When $\|\mathbf{w}\| \geq \epsilon$, $\dot{V} < 0$ as shown in the proof above with (92).

When $\|\mathbf{w}\| < \epsilon$, the term $2\mathbf{w}^T\boldsymbol{\eta}$ in Eq. (93) becomes (ignoring the factor 2)

$$\begin{aligned}\mathbf{w}^T\boldsymbol{\eta} &\leq \|\mathbf{w}\|\|\boldsymbol{\eta}\| \\ &\leq \rho\|\mathbf{w}\| \\ &= \rho\frac{\mathbf{w}^T\mathbf{w}}{\|\mathbf{w}\|}.\end{aligned} \tag{94}$$

Therefore,

$$\begin{aligned}\dot{V} &\leq -\mathbf{e}^T\mathbf{Q}\mathbf{e} + 2\mathbf{w}^T\left(\Delta\mathbf{v} + \rho\frac{\mathbf{w}}{\|\mathbf{w}\|}\right) \\ &= -\mathbf{e}^T\mathbf{Q}\mathbf{e} + 2\mathbf{w}^T\left(-\rho\frac{\mathbf{w}}{\epsilon} + \rho\frac{\mathbf{w}}{\|\mathbf{w}\|}\right).\end{aligned} \tag{95}$$

The maximum value of the second term is $\frac{\epsilon}{2}\rho$ when $\|\mathbf{w}\| = \frac{\epsilon}{2}$. Consequently,

$$\dot{V} \leq -\mathbf{e}^T\mathbf{Q}\mathbf{e} + \frac{\epsilon}{2}\rho < 0, \tag{96}$$

provided that

$$\mathbf{e}^T\mathbf{Q}\mathbf{e} > \frac{\epsilon}{2}\rho. \tag{97}$$

Using the relationship

$$\lambda_{\min}(\mathbf{Q})\|\mathbf{e}\|^2 \leq \mathbf{e}^T\mathbf{Q}\mathbf{e} \leq \lambda_{\max}(\mathbf{Q})\|\mathbf{e}\|^2, \tag{98}$$

$\dot{V} < 0$ if $\lambda_{\min}(\mathbf{Q})\|\mathbf{e}\|^2 > \frac{\epsilon}{2}\rho$, i.e.,

$$\|\mathbf{e}\| > \underbrace{\sqrt{\frac{\epsilon}{2\lambda_{\min}(\mathbf{Q})}}\rho}_{\equiv R}. \tag{99}$$

Let S denote the smallest level surface of V containing the ball B_R of radius R centered at $\mathbf{e} = 0$. If $\mathbf{e}(t_0) \in S$, then the solution remains in S. If $\mathbf{e}(t_0) \notin S$, then V is decreasing as long as $\mathbf{e}(t) \notin S$. ■

REFERENCES

Baruh, H. (1998). *Analytical Dynamics*. McGraw-Hill.

Bendtsen, J. D., Andersen, P., and Pedersen, T. S. (2002). Robust feedback linearization-based control design for a wheeled mobile robot. In *6th Int. Symposium on Advanced Vehicle Control (AVEC '02), Hiroshima, Japan*.

Brockett, R. W. (1983). Asymptotic stability and feedback stabilization. In *Differential Geometric Control Theory*, pages 181–191. Birkhauser.

Campion, G., Bastin, G., and D'Andrea-Novel, B. (1996). Structural properties and classification of kinematic and dynamic models of wheeled mobile robots. *IEEE Trans. on Robotics and Automation*, 12(1):47–61.

Corradini, M. L. and Orlando, G. (2001). Robust tracking control of mobile robots in the presence of uncertainties in the dynamical model. *J. of Robotic Systems*, 18(6):317–323.

D'Andrea-Novel, B., Campion, G., and Bastin, G. (1995). Control of nonholonomic wheeled mobile robots by state feedback linearization. *Int. J. of Robotics Research*, 14(6):543–559.

DeSantis, R. (1994). Path-tracking for a tractor-trailer-like robot. *Int. J. of Robotics Research*, 13(6):533–543.

Dixon, W., Dawson, D., Zergeroglu, E., and Zhang, F. (2000a). Robust tracking and regulation control for mobile robots. *Int. J. of Robust and Nonlinear Control*, 10(4):199–216.

Dixon, W. E., Dawson, D. M., and Zergeroglu, E. (2000b). Robust control of a mobile robot system with kinematic disturbances. In *Proc. IEEE Conf. on Control Applications*, pages 437–442.

Fang, H., Fan, R., Thuilot, B., and Martinet, P. (2006). Trajectory tracking control of farm vehicles in presence of sliding. *Robotics and Autonomous Systems*, 54(10):828–839.

Fierro, R. and Lewis, F. L. (1997). Control of nonholonomic mobile robot: Backstepping kinematics into dynamics. *J. of Robotic Systems*, 14(3):149–163.

Fliess, M., Levine, J., Martin, P., and Rouchon, P. (1995). Flatness and defect of non-linear systems: Introductory theory and examples. *Int. J. of Control*, 61(6):1327–1361.

Kim, M.-S., Shin, J.-H., Hong, S.-G., and Lee, J.-J. (2003). Designing a robust adaptive dynamic controller for nonholonomic mobile robots under modeling uncertainty and disturbances. *Mechatronics*, 13(5):507 – 519.

Laumond, J., editor (1998). *Robot Motion Planning and Control (Lecture Notes in Control and Information Sciences)*. Springer.

Leroquais, W. and D'Andrea-Novel, B. (1996). Modeling and control of wheeled mobile robots not satisfying ideal velocity constraints : the unicycle case. In *Proc. IEEE Conf. on Decision and Control*, pages 1437–1442.

Low, C. B. and Wang, D. (2007). Integrated estimation for wheeled mobile robot posture, velocities, and wheel skidding perturbations. In *Proc. IEEE Int. Conf. on Robotics and Automation*, pages 2355–2360.

Murray, R. and Sastry, S. (1991). Steering nonholonomic systems in chained form. In *Proc. IEEE Conf. on Decision and Control*, pages 1121–1126.

Pathak, K. and Agrawal, S. (2005). An integrated path-planning and control approach for nonholonomic unicycles using switched local potentials. *IEEE Trans. on Robotics*, 21(6):1201–1208.

Rouchon, P., Fliess, M., Levine, J., and Martin, P. (1993). Flatness and motion planning : The car with n trailers. In *Proc. European Control Conf.*, pages 1518–1522.

Ryu, J.-C., Agrawal, S. K., and Franch, J. (2008). Motion planning and control of a tractor with a steerable trailer using differential flatness. *ASME Transactions, Journal of Computational and Nonlinear Dynamics*, 3(3):031003.

Samson, C. and Ait-Abderrahim, K. (1991). Feedback control of a nonholonomic wheeled cart in cartesian space. In *Proc. IEEE Int. Conf. on Robotics and Automation*, pages 1136–1141.

Sarkar, N., Yun, X., and Kumar, V. (1994). Control of mechanical systems with rolling constraints: Application to dynamic control of mobile robots. *Int. J. of Robotics Research*, 13(1):55–69.

Seyr, M. and Jakubek, S. (2006). Proprioceptive navigation, slip estimation and slip control for autonomous wheeled mobile robots. In *Proc. IEEE Int. Conf. on Robotics, Automation and Mechatronics*, pages 1 – 6.

Sira-Ramirez, H. and Agrawal, S. K. (2004). *Differentially Flat Systems*. Marcel Dekker, New York.

Spong, M. W. and Vidyasagar, M. (1989). *Robot Dynamics and Control*. John Wiley & Sons.

Wang, Z. P., Su, C. Y., Lee, T. H., and Ge, S. S. (2004). Robust adaptive control of a wheeled mobile robot violating the pure nonholonomic constraint. In *Proc. IEEE Int. Conf. on Control, Automation, Robotics and Vision*, volume 2, pages 987–992.

Yang, J. and Kim, J. (1999). Sliding mode control for trajectory tracking of nonholonomic wheeled mobile robots. *IEEE Trans. on Robotics and Automation*, 15(3):578–587.

Zhang, Y., Chung, J. H., and Velinsky, S. A. (2003). Variable structure control of a differentially steered wheeled mobile robot. *J. of Intelligent and Robotic Systems*, 36(3):301–314.

Zhu, X., Dong, G., Hu, D., and Cai, Z. (2006). Robust tracking control of wheeled mobile robots not satisfying nonholonomic constraints. In *Proc. Int. Conf. on Intelligent Systems Design and Applications*, volume 2, pages 643–648.